Advances in Biology & Earth Sciences
Vol.4, No.2, 2019, pp.73-87

SIMULATION OF GROUND ACCELERATION ROUTES BY INTERPOLATION OF PGA DATA, WITHIN GUERRERO AND OAXACA STATES COASTAL BORDER, MEXICO

Fidel Martínez-García*

Vicente Guerrero, Colonia Las Granjas.
Cuernavaca, Morelos, Mexico

Abstract. In the scope of attenuation of seismic wave energy and seismic risk prevention, 17 earthquakes with a magnitude range 4.7 to 7.4 occurred from September 2012 to February 2017, in the southern of the Mexican Republic within the Guerrero and Oaxaca states coastal limits were analyzed. The study focus was the data spatial analysis behavior of the peak acceleration, PGA (cm/s^2), and the response of the continental and maritime mass to the transit of seismic waves, considering distance to the epicenter and hypocenter; the composition and the rock structure; besides the effect of size, saturation, weathering and mineral content on the integrity of materials, all as factors that determine the intensity of seismic waves. Derived from the analysis data, three maps that show the simulation of seismic waves passage are included; resulting maps, show spatially the possible routes that follow the seismic waves; the continental mass impact; the priority areas where it would be necessary to perform a seismic risk analysis; aside from possible physical causes of the intensity changes of the seismic waves in remote regions more than 300 kilometers away from the epicenters, areas where intensities greater than the IV degrees on the Mercalli scale have been perceived.

Keywords: *Cocos Plate, epicenter, North American Plate, peak ground acceleration, seismic risk analysis, wave energy attenuation.*

****Corresponding Author:*** *Fidel Martínez-García, Vicente Guerrero, Colonia Las Granjas. Cuernavaca, Morelos, Mexico, C.P. 62460, Tel.: +52 7772553462, e-mail: Eco599395@gmx.com*

***Received**: 14 May 2019;* ***Accepted**: 10 June 2019;* ***Published**: 10 August 2019.*

1. Introduction

When an earthquake occurs, there are three important characteristics that distinguish it in relation to the release of energy and the magnitude: the distance to the focus or hypocenter; its epicenter, and its intensity. According to the third distinctive feature of the phenomenon, a building emplaced on solid rock will suffer less damage than a building constructed on a bed of sand.

The rocks at their most intimate essence, are formed by grains of one or more minerals and their composition and atomic structure are determinants of their physical qualities and their form, in particular the crystalline structure and the strength of chemical bonds (Boutrid *et al.*, 2015). Such qualities, without doubt, intervene in their hardness and how they respond when subjected to high temperatures, pressures and squeeze within the lithosphere or within the upper mantle during tectonic activity.

In the opinion of geophysicists, in solid rock formations generally quake less than in sand formations, but such a claim is not so true when analyzing the local natural conditions of sites surrounding where an earthquake was perceived. The versatile hardness of the rock and the physical characteristics such as size, saturation, weathering and mineral content, influence the compressive strength of rock materials (Johnston, 1979; Agustawijaya, 2007; Ehlen, 2002), they are factors determinant so that seismic waves increase their intensity when they propagate from the hard rock mass to the soft ground or when the seismic waves overlap.

The strength of the movements of the earth's crust after an earthquake depends largely on the structure of the rock masses near the surface. Generally, the earthquake strongly on surfaces where the local substrate is soft and vice versa; similarly, some deep parts of the Earth also contribute to certain areas shaking more strongly. This happens because seismic waves increase in intensity when they propagate from the hard rock mass to the soft substrate. They also increase their intensity when the deviated waves and reflected waves overlap, such as occurs in the lake area where Mexico City sits, which is characterized by highly compressible clay deposit, highly hydrated and supported by resistant sands (Singh *et al*., 1987).

The interaction between human population and the seismic areas is mainly with the frequent movement of the earth's crust, which can be very weak until destructive, and even catastrophic. However, the severity of the affectations is also determined by the distance to the epicenter and hypocenter, the depth and the characteristics of the landmass where the seismic waves cross. This interaction of that factors theoretically attenuates the movement and contributes to the decrease of mechanical energy as the potentially affected populations are more away from the phenomenon; this attenuation or decrease in mechanical movement has been estimated by empirical equations based, for example, on the linear regression (Chávez *et al*., 2012; García-Soto *et al.*, 2012).

Seismic waves move people and objects in all directions because of the acceleration or changes in the velocity of the ground, whose duration and strength depend on the frequency of the seismic waves at a certain point, being more perceptible according to the proximity to the epicenter. Beyond the maps made in Mexico City and other small cities in the Mexican province (Cortés-Niño & Sánchez-Tizapa, 2017), the small-scale mapping of the records obtained from seismic waves in accelerometers are generalizations. Data that aim to provide sufficient information for the decision making of the competent authorities and builders in the design and application of construction regulations within the framework of integral seismic risk management (Sandoval *et al*., 2012). However, this purpose is not fulfilled as it does not show, for example, priority areas where seismic waves amplify their intensity after the nature of the substrate changes, causing the waves to be deflected and reflected inducing they overlapping, very frequent in valleys and depressions (Tsige & García Flórez, 2006).

The shake maps provided by the National Seismological Service (SSN) of Mexico, reflect the automated generic interaction of a phenomenon (hypocenter, epicenter, distance and intensity) from the perspective of numerical analysis using algorithms and rigid mathematical rules (Chávez *et al*., 2012; Sandoval *et al*., 2012), Figure 1, but they do not visually reflect, under conditions as real as possible, the interaction and attenuation resulting from seismic waves (force, direction, superposition) with the earth's mass (saturation, hardness, depth, discontinuity, among others) (Johnston *et al*., 1979; Chávez *et al.*, 2012).

The data of peak acceleration (PGA-SSN) collected in the accelerometers when recording the waves data coming from an earthquake, reflect in some way that interaction, they are an underestimated timely index that summarizes what happens in the periphery with nearby seismic waves and different types of rock mass; this information combined with thematic information, could make possible to generate a complementary map that evidences the priority areas where it is necessary to carry out an analysis of seismic risk or the construction materials must be reinforced by applying better methods (Syed Mohsin *et al*., 2018).

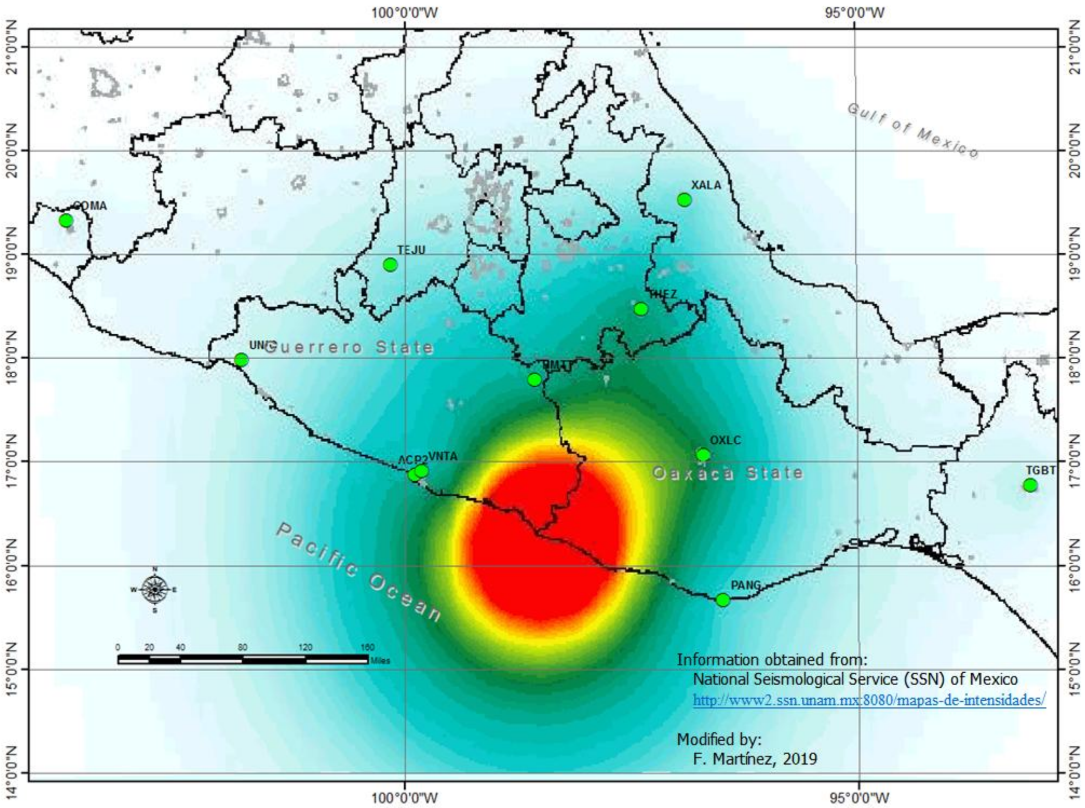

Fig. 1. Characteristics of the maps published by the National Seismological Service after the manifestation of an earthquake, the image corresponds to the event of March 20, 2012

2. Background

According to the data obtained from the catalog of earthquakes of the National Seismological Surby of Mexico (to the south of the Mexican Republic, from September 2012 to February 2018, there were 17 earthquakes with a magnitude range of 4.7 to 7.4, being undoubtedly two events the most important of that period due to its proximity to Mexico City. The 17 events chosen were originated near the coast in the continental territory in the south of the country between the coastal and territorial limits of the Guerrero and Oaxaca states, a very active tectonic region due to the subduction phenomenon of the Cocos Plate under the North American Plate, region with a very complex tectonic history of repeated folding events, magmatism and metamorphism whose metamorphic rocky basement is represented by the Xolapa complex (Yamamoto *et al*., 2013), (Perez-Gutierrez *et al*., 2009).

For the seismic record, in the national scope, Mexico has a seismic broadband network that consists of 61 stations that collect information on the seismic events that occur in the Trans-Mexican Volcanic Belt and on the Pacific Ocean coasts and the State of Veracruz (http://www.ssn.unam.mx/acerca-de/estaciones/) (Quaas *et al*., 1996). The stations consist of a seismometer that records the seismic waves in a wide band of frequencies and magnitudes, in addition to an accelerometer that registers changes of direction of the ground within a wide frequency spectrum for large, local and regional earthquakes; of local scope the seismological network is complemented with 41 equipment that registers data in very specific places, in example, Colima volcano and Popocatepetl volcano.

The world seismic records history can be considered very recent and is not yet enough to identify the earth's seismic cycles, in view of this reality the general consensus in the field of geology, engineering, seismology and geophysics is that earthquakes cannot be predicted, therefore a seismic eventuality of a specific area is regularly calculated mathematically considering: a) the modeling of the occurrence of an earthquake, b) the seismic-genetic zones, c) the magnitude-recurrence relationships, and d) the laws of attenuation based on the prediction of ground movement (García-Soto *et al.*, 2012). In the field of attenuation, the study of real conditions regularly receive slight importance according to what the recorded values of PGA (cm/s^2) reveal in the stations of the seismological network, considering that along the route that follow the seismic waves from the hypocenter and epicenter, the variations of the rock formations, horizontally and vertically, are countless. The truth is that the real response that the land mass has to seismic waves can be considered with a high degree of uncertainty since the data obtained by the stations only reflect what happens in the immediate periphery of the instrumented area but not what happened during the path of the waves; undoubtedly the local response could be conditioned and depend on the nature, state, volume and variation of the rock, and not always on the horizontal and vertical distance of the site where the phenomenon occurs, (Chávez *et al*., 2012; Singh *et al*., 1987; Cortés-Niño & Sánchez-Tizapa, 2017; Sandoval *et al.*, 2012).

The focal point of this research is to generate interactive attached maps through the spatial analysis of the data recorded in the accelerometers in response to an earthquake. The analysis of the data of 17 earthquakes in 68 stations is carried out, considering the spatial variations of PGA (cm/s^2) (peak ground acceleration) recorded in the accelerometers, Figure 2. The analysis is limited to a simplified study by means of the representation or mapping, of the spatial behavior of PGA data and the response of the maritime - terrestrial mass to the seismic wave transit.

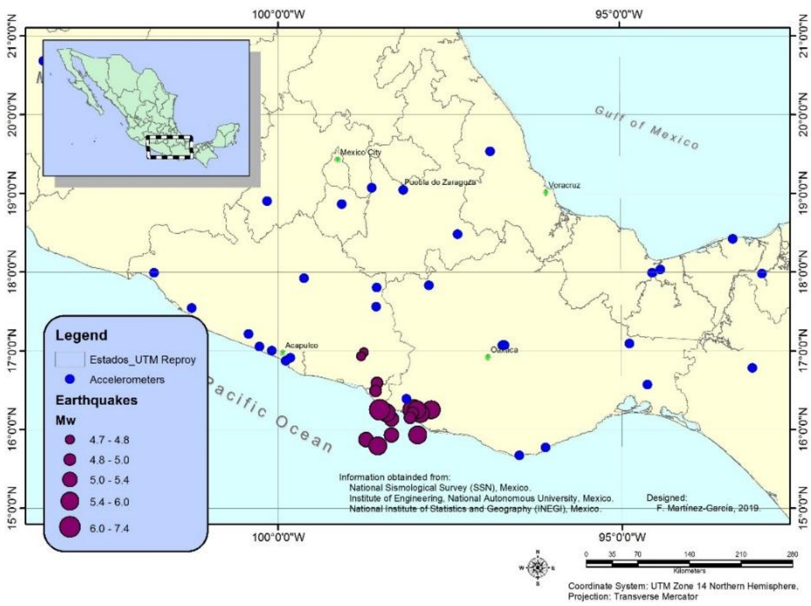

Fig. 2. Study area geographical representation

3. Methodology

By consulting the National Seismological Service website, tabulated data from 17 seismic events occurred from March 2012 to February 2018 were collected, with a magnitude of 4.7 to 7.4; the data were extracted from the catalog of earthquakes (http://www2.ssn.unam.mx:8080/catalogo/), giving emphasis to nine earthquakes that occurred in the continental area or very close to it.

The peak ground acceleration data for each of the earthquakes (map of intensities or PGA in KMZ format), were obtained from 66 stations by consulting the following web pages of the National Seismological Service (Quaas *et al*., 1996) and the Institute of Engineering of the National Autonomous University of Mexico:

http://www2.ssn.unam.mx:8080/mapas-de-intensidades/ and
http://aplicaciones.iingen.unam.mx/AcelerogramasRSM/Registro.aspx

Each intensities information maps was edited with the “Global Mapper GIS application”, generating and exporting two point files in "SHP" format corresponding to the registration stations and epicenters, as well as a file in the "GeoTIFF" format. The tools used for data export were "Export Raster / Image format" and "Export Vector / Lidar format". In addition, a table was integrated with data on date, time, geographic location, depth and magnitude of the 17 events; the table was edited in the Excel spreadsheet and subsequently converted to plain text format in order to be re-projected in a GIS environment (Blue Marble Geographics, 2015).

The export options with the Global Mapper (TM) GIS application of the GeoTIFF images considered a type of 24 bit RGB image, sample Spacing / scale for the geographical coordinates x, y; and DPI values of 300 to obtain the best possible resolution. The resulting layers of the peak ground acceleration data (GPA) and images of the earthquakes were added as a data set to maps in the geographic platform of ArcGis™, 2015, through the corresponding numerical fields (Blue Marble Geographics, 2015) .

The topography and geology data were obtained from the vector data set referred to in the following National Institute of Statistics and Geography (INEGI) web pages.

http://www.beta.inegi.org.mx/temas/mapas/geologia/
http://www.beta.inegi.org.mx/temas/mapas/topografia/

they corresponded to 22 thematic charts of faults and fractures in "SHP" format, scale 1: 250000 with the cartographic keys: F13-12, E13-3, E13-6-9, F14-10, E14-1, E14-4, E14-7-10, E14-2, E14-5, E14-8, E14-11, E14-3, E14-6, E14-9, E14-12, D14-3, E15-1-4, E15- 7, E15-10-D15-1, E15-5, E15-8, E15-11.

The thematic representation of the continental barriers or land mass that simulate the opposition to the passage of seismic waves, were obtained of level curves extracted from the topography data of the INEGI vector data set, referred to above.

The characteristics of the surrounding lithology of the land mass on which the seismic wave recording stations are established; were obtained from the Mexican Geological Survey, SGM (https://www.gob.mx/sgm), they also corresponded to 22 digital charts in PDF format in scale 1: 250000 of the geological-mining class with the same keys of the INEGI cartographic base referred to above. Each digital chart in PDF format was rectified with the Global Mapper GIS application using the “Image Rectifier tool” and then exported with GeoTIFF format (Blue Marble Geographics, 2015).

With a base map composite of INEGI vector data integrated of the epicenters, state borders, continental barriers and stations layers and the peak acceleration records, PGA (cm/s^2), of the National Seismological Service, within the ArcGis platform, by interpolation four maps were created. The interpolation process uses a raster surface, using barriers, from the points (PGA) using a spline technique of minimum curvature. The simulation of continental barriers was introduced as polyline elements. The detailed description of the process of "Spline with barriers" can be consulted in the following link of the “ArcGIS 10.1 tool help”, https://resources.arcgis.com/en/help/main/10.1/index.html#//009z00000079000000

4. Results

In Table 1 a list the 17 earthquakes used for the information analysis is included, all of them occurred between the states of Guerrero and Oaxaca during the period from March 2012 to 2018, of which two earthquakes stand out, one of March 20 of 2012, with epicenter located to the south of the Ometepec municipality, Guerrero state, its magnitude was of 7.4 occurred at 16 km depth; the epicenter was located in the continental area but very close to the coast, it was an interplate event with an inverse type fault mechanism. Another important earthquake occurred on February 16, 2018, to the south of the Pinotepa Nacional municipality, Oaxaca state, also within the continental area; had a magnitude of 7.2 occurred at a 12 km depth, also corresponded to an interplate event with a focal mechanism of inverse fault (Aguirre-González & Rodríguez-González, 2012; SSNMEX, 2018; UIS-UNAM, CIS-IIGEN, & FCT-UALN, 2018), both seismic events happened in the contact area of the Cocos plate and the North American plate, tables 2-3 summarize the characteristics of the referred earthquakes.

Table 1. Main earthquakes occurred between the coastal states limits of Guerrero and Oaxaca from 2012 and 2018

No	Date	Time	LN	LW	Geographic location	Mag.	Depth (km)
1	20/03/2012	12:02:47	16.42	-98.36	29 km S of Ometepec, Gro. State	7.4	16
2	06/08/2013	15:17:30	16.49	-98.58	28 km SW of Ometepec, Gro. State	5.1	16
3	24/05/2014	03:24:45	16.21	-98.42	42 km SW of Pinotepa Nal., Oax. State	5.7	18
4	13/08/2014	01:48:11	16.13	-98.35	40 km SW of Pinotepa Nal., Oax. State	5.4	10
5	09/03/2014	18:37:57	15.79	-98.55	82 km SW of Pinotepa Nal., Oax. State	5.8	16
6	07/12/2015	03:44:07	16.98	-98.75	50 km to NW of Ometepec, Gro. State	4.7	46
7	29/09/2015	23:44:44	16.93	-98.79	49 km to NW of Ometepec, Gro. State	4.8	31
8	25/06/2015	05:31:46	16.15	-98.08	22 km S. of Pinotepa Nal., Oax. State	5.0	16
9	27/06/2016	15:50:33	16.2	-97.93	20 km SE of Pinotepa Nal., Oax. State	5.7	20
10	08/05/2016	02:33:59	16.25	-97.98	13 km SE of Pinotepa Nal., Oax. State	6	35
11	23/03/2016	18:29:38	16.21	-98.04	15 km South of Pinotepa Nal., Oax. State	4.9	10
12	20/12/2017	21:23:33	15.93	-98.35	56 km SW of Pinotepa Nal., Oax. State	5.2	16
13	12/01/2017	04:26:57	16.59	-98.56	19 km SW of Ometepec, Gro. State	5.0	40
14	20/03/2018	11:46:53	15.87	-98.72	88 km SW of Pinotepa Nal., Oax. State	5.3	13
15	19/02/2018	00:56:57	16.25	-97.77	32 km SE of Pinotepa Nal., Oax. State	6.0	10
16	16/02/2018	18:36:52	15.93	-97.97	46 km S of Pinotepa Nal., Oax. State	5.9	16
17	16/02/2018	17:39:38	16.25	-98.03	11 km S of Pinotepa Nal., Oax. State	7.2	12

Table 2a. Characteristics of first EQ important event occurred to the south of Ometepec, Guerrero state, in March 20, 2012

Station Key	PGA	Intensity	Distance (km)	Altitude	Surrounding geol. faults *	Geology	UCS
JAMI	293.51	Strong	59.53	481	3	Granodiorite	200
COPL	68.28	Moderate	69.85	32	1	Granite-Granodiorite	275
RIOG	40.85	Moderate	108.23	27	1	Alluvium	20
OZST	38.49	Moderate	301.64	1244	10	Lahar and sandstone	95
OXAL	37.51	Moderate	188.12	1554	1	Alluvium	20
OXLC	37.17	Moderate	190.53	1542	1	Alluvium	20
SCT2	36.99	Moderate	339.54	2240	0	Alluvium	20
SAPP	36.47	Moderate	292.25	2173	1	Lahar and andesitic tuff	125
ACAZ	36.17	Moderate	157.90	10	1	Alluvium	20
TOTO	33.94	Moderate	322.18	2290	0	Lacustrine	20
ACAR	30.33	Moderate	165.62	10	0	Metamorphic complex	140
THEZ	30.13	Moderate	250.19	1631	10	Polymictic conglom.-travertine	140
RFPP	26.82	Moderate	290.82	2139	1	Lahar and andesitic tuff	125
OXBJ	26.77	Moderate	188.59	1567	1	Alluvium	20
GALE	26.26	Moderate	205.80	1260	1	Metamorphic complex	140
LANE	26.00	Moderate	135.85	16	0	Metamorphic complex	140
CSER	25.43	Moderate	302.77	2956	0	Basalt	300
MIHL	24.63	Moderate	441.77	21	0	Sandstone and conglomerate	140
ACP2	23.62	Moderate	170.37	151	1	Granite-Granodiorite	275
SXPU	23.46	Moderate	290.28	2181	1	Lahar and andesitic tuff	125
POZU	22.80	Moderate	151.30	357	2	Metamorphic complex	140
HMTT	21.85	Moderate	153.96	898	1	Alluvium	20
PBP2	21.81	Moderate	290.93	2149	1	Lahars and andesitic tuff	150
SRPU	19.84	Moderate	281.83	2114	1	Lahars - sandstones	95
PZPU	19.20	Moderate	291.92	2206	1	Lahars and andesitic tuff	150
OXJM	18.72	Moderate	311.47	158	1	Granodiorite	200
PHPU	18.63	Moderate	291.06	2172	1	Lahars and andesitic tuff	150
RABO	17.44	Moderate	237.94	1279	0	Lahars	40
FEPP	14.43	Moderate	286.16	2132	1	Lahars and andesitic tuff	150
CUP5	13.98	Moderate	333.52	2240	0	Basalt	300

PGA = Peak Ground Acceleration; UCS = Unconfined Compressive Strength; * total faults per site distributed from 1 to 10.

Figures 3-4 show the results of the interpolation process described in the methodology with the aim of obtaining a regional map showing the routes followed by mechanical energy and the possible land mass barriers that moderate its movement; the prediction of values from the data used correspond to the peak acceleration recorded in the stations referred to in tables 2 – 3: 66 data for the seismic event of March 20, 2012 and 24 data for the seismic event of February 16, 2018.

Table 2b. Characteristics of first EQ important event occurred to the south of Ometepec, State of Guerrero, in March 20, 2012

Station Key	PGA	Intensity	Distance (km)	Altitude	Surrounding geol. faults *	Geology	UCS
AGCA	13.87	Moderate	144.64	31	2	Metamorphic complex	140
CHFL	13.84	Moderate	179.31	1716	1	Polymictic conglom. - sandstone	140
TNLP	13.39	Moderate	225.06	734	2	Sandstone - Shale	150
COYC	13.02	Moderate	195.20	26	2	Granite-Granodiorite	275
TEAC	12.32	Moderate	269.44	978	1	Lahars - sandstones	95
SODO	12.30	Moderate	356.26	101	0	Lahars - sandstones	95
TACY	12.08	Moderate	341.84	2240	0	Alluvium	20
OCLL	11.46	Moderate	175.65	710	1	Metamorphic complex	140
BHPP	10.80	Moderate	297.90	2171	1	Lahar and andesitic tuff	125
SJLL	10.70	Moderate	30.17	46	1	Metamorphic complex	140
VNTA	10.02	Moderate	164.89	50	1	Metamorphic complex	140
HUAM	8.88	Moderate	290.84	91	1	Volcano - Sedimentary	140
PANG	7.93	Moderate	216.72	20	1	Metamorphic complex	140
CAYR	7.65	Moderate	214.88	19	0	Metamorphic complex	140
XALA	7.19	Moderate	377.20	1374	1	Basalt	350
SCRU	7.00	Moderate	337.84	87	0	Granite-Granodiorite	275
TEJU	5.74	Moderate	334.61	1340	1	Schist - Chert	70
COMD	5.54	Moderate	297.27	306	1	Polymictic conglomerate	140
ATYC	5.53	Moderate	237.61	51	1	Granite-Granodiorite	275
VHSA	5.33	Moderate	602.90	23	0	Alluvium	20
NILT	5.05	Moderate	400.22	65	1	Alluvium	20
LMPP	4.69	Slight	286.24	2140	1	Lahars and Andesitic tuff	150
SCCB	4.57	Slight	476.08	2137	1	Granodiorite	200
ACAM	4.06	Slight	472.01	1858	1	Rhyolite - Rhyolitic tuff	175
SNJE	3.97	Slight	392.18	182	1	Granodiorite	200
TGBT	3.91	Slight	564.59	585	2	Limestone - Shale	200
URUA	3.78	Slight	514.94	1664	1	Andesite - Basalt	250
COYQ	3.45	Slight	306.23	44	2	Granite-Granodiorite	275
NUX2	3.13	Slight	273.64	10	1	Granite-Granodiorite	275
SLPA	2.72	Slight	418.29	2591	3	Andesite - Dacite	250
SLU2	2.64	Slight	290.45	29	1	Granite-Granodiorite	275
CANA	2.47	Slight	451.65	340	1	Dacite - Rhyolite	175
UNIO	2.31	Slight	405.92	56	1	Sandstone - Limestone	200
CDGU	1.27	Slight	649.69	1583	2	Piroclasts	140
CALE	1.16	Slight	501.90	10	1	Sandstone - Limestone	200

PGA = Peak Ground Acceleration; UCS = Unconfined Compressive Strength; * total faults per site distributed from 1 to 10.

Table 3. Characteristics of second EQ important event occurred to the south of Pinotepa National, State of Oaxaca, in February 16, 2018

Station Key	PGA	Intensity	Distance (km)	Altitude	Surrounding geol. faults *	Geology	UCS
ACAM	2.44	Slight	506.9	1858	7	Rhyolite - Rhyolitic tuff	175
ACP2	18	Moderate	209.8	151	0	Granite-Granodiorite	275
ATYC	7.96	Moderate	277.4	51	3	Granite-Granodiorite	275
COMA	3.57	Slight	696.7	606	2	Alluvium	20
COYC	7.68	Moderate	234.8	26	0	Granite-Granodiorite	375
HLIG	12.3	Moderate	176.5	1744	0	Polymictic conglom. - sandstone	140
HMTT	21.2	Moderate	180.3	898	1	Alluvium	20
MEIG	15.2	Moderate	250.9	553	10	Sandstone-Shale	150
MIHL	9.72	Moderate	418.2	21	2	Sandstone and polymictic conglom.	200
NILT	4.8	Moderate	366.5	65	1	Alluvium	20
OXBJ	27.1	Moderate	166.1	1567	1	Alluvium	20
PET2	2.4	Slight	372.5	45	2	Granite-Granodiorite	275
PHPU	23.9	Moderate	309.5	2172	3	Lahar and andesitic tuff	150
PNIG	192	Strong	18.9	247	0	Metamorphic complex	140
PPIG	17.2	Moderate	318.1	3997	4	Andesite - Dacite	375
TEJU	3.41	Slight	370.5	1325	4	Schist - Slate	40
TGBT	2.7	Slight	531.5	602	5	Limestone and shale	200
TLIG	15.7	Moderate	156.1	1084	0	Limestone	180
TPIG	10.6	Moderate	250.4	1460	10	Polymictic conglom. - Travertine	140
TUIG	5.11	Moderate	432	7	2	Alluvium	20
UNIO	2.41	Slight	445.8	56	1	Limestone	120
VHSA	2.67	Slight	575.6	23	2	Sandstone and polymictic conglom.	200
VNTA	6.12	Moderate	204.5	30	1	Metamorphic complex	140
XALA	5.93	Moderate	382.2	1374	1	Basalt	300

PGA = Peak Ground Acceleration; UCS = Unconfined Compressive Strength; * total faults per site distributed from 1 to 10.

5. Discussion

Given the dilemma that earthquakes are unpredictable in time and space, prevention is the best alternative to anticipate the damage caused, a proper planning and good mitigation and construction practices are needed (Ma'hood *et al.*, 2009), so it is imperative to have additional information that guides to identify the areas where these phenomena cause more disaster. Since the 1985 earthquake occurred on September 19, 1985 on the coasts of Michoacán, the methods of construction of the housing infrastructure have been more efficient to resist the waves and accelerations that subsequent earthquakes could cause, but even so apparently it has not been enough due to the experience left by the earthquake of September 19, 2017 (Torres-Álvarez, 2017).

Undoubtedly, Mexico City has been one of the most studied cities due to the characteristics of the subsoil where it is located, which contributes to the seismic waves that arrive in this area modifying their intensity by being diverted and reflected, resulting in an overlap and amplification of its signal in several magnitude levels (Singh *et al.*, 1987; Tsige & García Flórez, 2006).

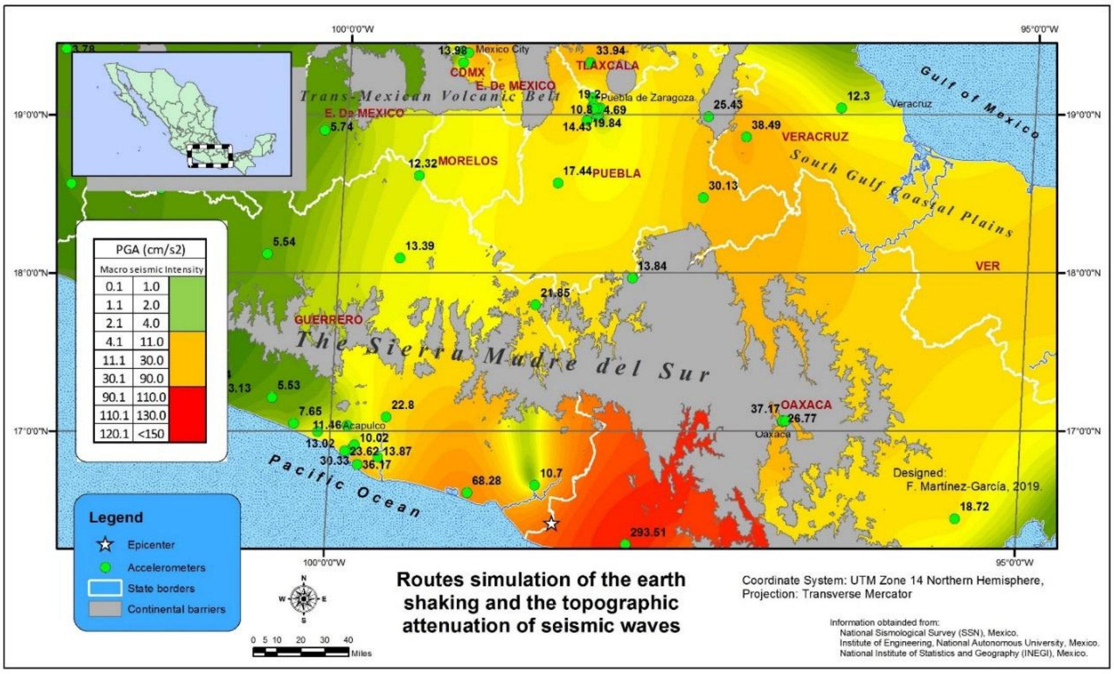

Fig. 3. Spatial prediction of values from the peak ground acceleration data recorded at 66 stations for the seismic event of March 20, 2012

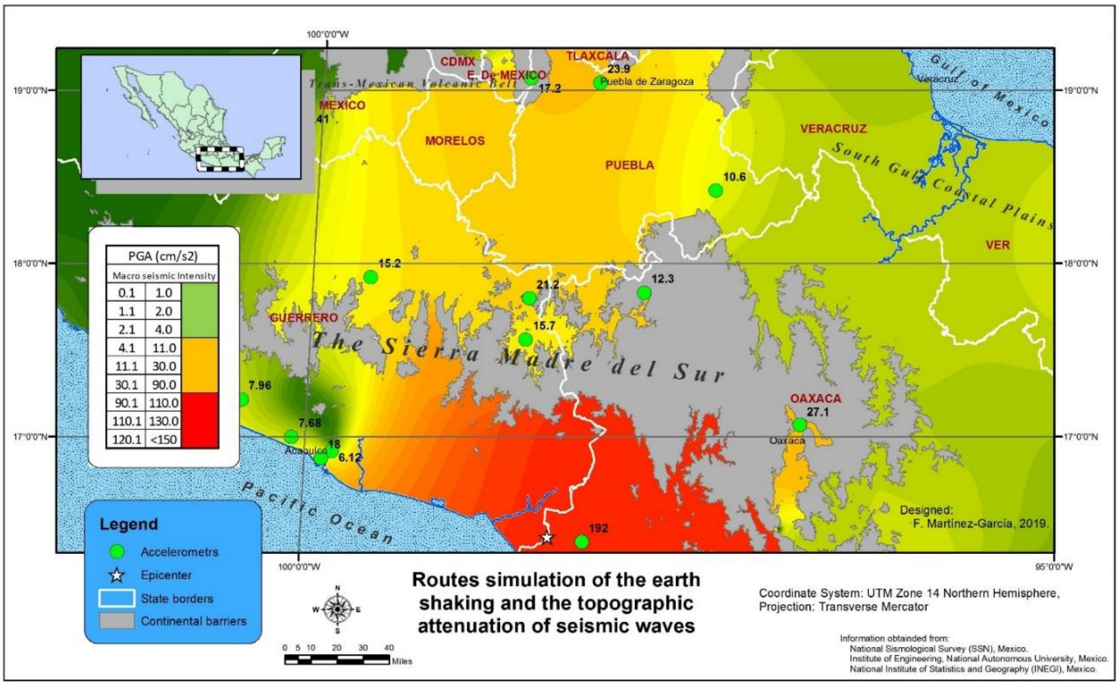

Fig. 4. Spatial prediction of values from the peak ground acceleration data recorded in 24 stations for the seismic event of the February 16, 2018

This condition gives clear evidence that the characteristics of the rock and the interaction they have with seismic waves from earthquakes with magnitudes greater than 6 Mw, is not irrelevant (Torres-Álvarez, 2017; Álvarez-Rubio, 1999).

The uncertainty that represents determining the real response that the earth's mass has to the seismic waves around the instrumentation area, shows that it is conditioned to the nature, state, volume and variation of the superficial rock and deep layers (Chávez *et al*., 2012; Singh *et al*., 1987; Cortés-Niño & Sánchez-Tizapa, 2017; Sandoval *et al*., 2012). This is corroborated with the analysis of the recorded acceleration data in seven stations located in the center of the Puebla city, in a square area of 6 by 2 kilometers (Stations PBP2, PHPU, PZPU, RFPP, SAPP, SXPU), during the seismic event of March 20, 2012, a range of variation at peak acceleration was from 4.69 to 36.47 PGA (cm/s^2), table 2a.

Seismic waves do not radiate in immutable concentric circles when they reach the earth's surface such as what is observed in a body of water by throwing a stone inside. Whenever seismic waves interact with the earth's surface and continental barriers change its direction and intensity what dissipates or increases their energy when interact with the rock mass which varies its nature due to the presence of fluids, degree of saturation, porosity, pressure and mineral content (Raji, 2013). The attenuation due to the distance to the hypocenter is determined by the pressure and temperature by the effect it has on the closure of fractures in the rock (Morales-Corona & Ramírez-Herrera, 2012).

In the same way, the amplitude of the wave decreases with the distance to the earthquake (vertically and horizontally); this decrease and how fast it occurs when interacting with the state of the rock, mineral composition and physical state, has allowed to describe also the structure of the Earth (Völgyesi, 1982) or also the presence of reservoirs of hydrocarbons (Raji, 2013), all this information has also been fundamental for the design of earthquake resistant structures and seismic warnings (Cormier, 2011).

According to the interpretation of the peak acceleration data (PGA) obtained from the SSN and the maps generated by interpolation, they show that the spatial distribution of the interpolated data prediction has important interactions with the regional geography, Figure 5. The epicenters of the earthquakes of greater magnitude registered in the study area (7.2 to 16 km of depth and 7.4 Mw to 12 km of depth), correspond in general to alluvial plains of the coastal zone. However, at 35 kilometers to the North of the epicenters there are already elevations higher than 2600 masl (local mountains) that attenuate their speed; these seismic events exhibited the acceleration data, PGA (cm/s^2), highest with 293.51 in the JAMI station and 190 PNIG in the OXCL station, figures 2 - 4, with the most outstanding data of the 17 events occurred during the period study.

When considering the combination of PGA values in the study area of all the stations that recorded data for the two main events (figures 4 and 5), the greater local physiographic influence that immediately contributes to the attenuation of the seismic waves of these two events is the Sierra Madre del Sur, is a mountain range in southern Mexico, extending 870 kilometers from southern Michoacan East through Guerrero state, to the Isthmus of Tehuantepec in eastern Oaxaca state.

Contrary in the depression of the Balsas river and valleys within the state of Guerrero and Oaxaca, which collaborate and intensify the intensity of the seismic waves; another region that increases the intensity of seismic waves is largely the area of the states of Puebla and Morelos with a small portion of the state of Veracruz due to the presence of valleys and scattered hills.

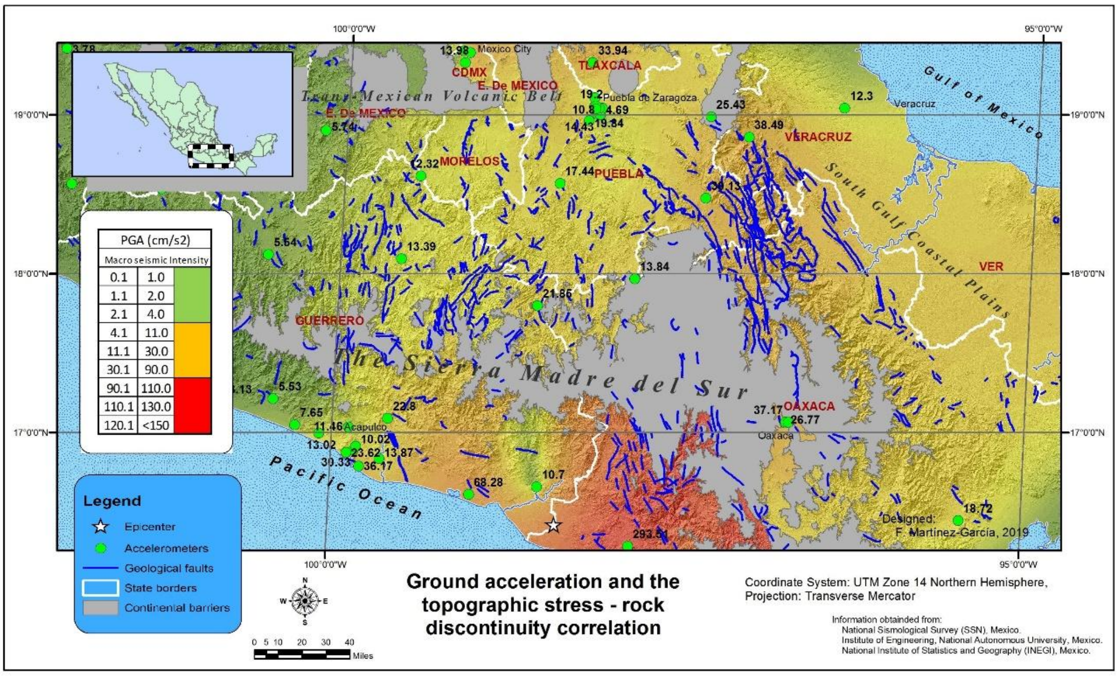

Fig. 5. Effect of mass rock discontinuity and the increment of PGA

Although in smaller proportion, another area that also increase the amplification of seismic waves in the Tepalcatepec River depression, located between the states of Michoacán and Guerrero states, Figure 4.

6. Conclusions

The variability of the rock and physical characteristics such as size, saturation, weathering and mineral content influence the compression and strength of the rock mass; these factors determine the seismic wave intensity and their permanence when they propagate inside the Earth or on its surface. Under this reasoning and derived from the information provided by the earthquake of March 20, 2012, it is now known that in the region of the continental margin of Ometepec, Guerrero state, the seismic activity is unusual since the local area is fractured in several blocks that move independently (Yamamoto *et al*., 2013), Figure 5.

When earthquakes are generated in the maritime environment, the main protective barrier that contributes to mitigate their frequency and amplitude is undoubtedly the maritime mass, but the main risk associated is the formation of tsunamis. In the recent history of Mexico, the most important event of this nature recorded in the Mexican coasts corresponds to that occurred on the beaches of Colima on June 22, 1932, which is attributed to a behavior generated by an underwater landslide and is considered one of the most destructive events of the epoch (Núñez-Cornú *et al*., 2008; Okal & Borrero, 2011). However, there were another important event occurred in 1787 that could have affected low areas in a coastal strip of 278 kilometers from the Acapulco bay to Salina Cruz bay (Núñez-Cornú *et al*., 2008). This water movement was related to a telluric event with an estimated magnitude of 8.6 generated in the Oaxaca coasts (Núñez-Cornú *et al*., 2008).

The immediate attenuation of the energy of earthquakes generated in the earth's environment is closely related to natural barriers and the distance to the hypocenter and epicenter, therefore the most destructive are the superficial events <5 Mw; therefore in a circular range of 130 km and according to the depth at which they occurred, the earthquakes of March 20, 2012 and February 16, 2018, correspond to this category.

Nowadays the degree of sensory perception used to quantify the effects of an earthquake on the surface is not the only source of information, at the present time the information is obtained from the seismological stations and its accelerometers incorporated, but the acceleration data registered in each station when an earthquake occur are still incidental and surely the surrounding orography has contributed to intensify or diminish its energy, therefore it is desirable to deepen in the studies of the local amplification effects, radiation patterns and directivity of seismic waves (Aguirre-González & Rodríguez-González, 2012), as well as the integrating the regional geological features of the site.

Certainly seismic waves of earthquakes with magnitudes greater than 6.5 Mw travel great distances but sometimes their spatial distribution is atypical; the effects of the earthquake of March 20, 2012 were felt with intensity VI on the scale of Mercalli in Orizaba and Ixtaczoquitlán, Veracruz (station OZST: 38.49 cm/s^2) 380 kilometers from the epicenter, an event considered unusual because of the damage it caused (Aguirre-González & Rodríguez-González, 2012), the place referred is located in a quaternary environment of lahar and sand, within the influence area of the Gulf coastal plain of Mexico where has been identified some gas reserves and petroleum bearing of shale, rock that is regularly breaks easily, (Mártir-Mendoza, 2014), Figure 5.

Large areas of Mexico, to north, south and SE of the Trans-Mexican Volcanic Belt, as well as coastal regions adjoining the Gulf of Mexico and the Pacific Ocean, are occupied by the important human populations; these outlying areas are characterized by quaternary alluvial soils, conglomerates and lahars, among the most important are to mention "The Oaxaca Central Valleys ", "The Anahuac Valleys ", "The Tepalcatepec River depression", "Coasts and coastal plains” (Veracruz , Guerrero, Oaxaca, Jalisco, Colima), extensive areas of the "The Balsas River depression ".

These broad areas usually receive the onslaught of waves of low amplitude but because of the terrain conditions tend to increase their intensity despite the distance, being comparable to amplitudes that occur at the epicenter site (Tsige & García Flórez, 2006), for example, as it happened in Mexico City or the case of Ixtaczoquitlán, Veracruz during the earthquake of March 20, 2012.

References

Aguirre-González, J. & Rodríguez-González, M. (2012). El sismo del 20 de marzo de 2012 en su exacta dimensión. *Geotécnia*, *2012*, 37–38. Retrieved from: https://www.smig.org.mx/archivos/revista-trimestral-smig/revista-geotecnia-smig-numero-224.pdf

Agustawijaya, D.S. (2007). The Uniaxial Compressive Strength of Soft Rock. *Civil Engineering Dimension*, *9*(1), 9-14. Retrieved from: http://puslit2.petra.ac.id/ejournal/index.php/civ/article/view/16584

Álvarez-Rubio, S. (1999). El efecto local sobre el movimiento sísmico del suelo: fenomenología y resultados recientes. *Física de La Tierra*, *0*(11), 141–173. Retrieved from: http://revistas.ucm.es/index.php/FITE/article/view/FITE9999110141A/12085

Boutrid, A., Bensihamdi, S., Chettibi, M. & Talhi, K. (2015). Strength hardness rock testing.

Journal of Mining Science, *51*(1), 95–110. https://doi.org/10.1134/S1062739115010135

Chávez, A.C., Arroyo, G.M., Zúñiga, R., Figueroa, A., Pérez, M.A. & López, C.S. (2012). Relación de atenuación del movimiento del suelo para la aceleración máxima (PGA) sobre el cinturón volcánico mexicano (MVB); análisis por trayectoria. *Revista de Ingeniería Sísmica*, *93*(87), 67–93. Retrieved from: http://www.scielo.org.mx/pdf/ris/n87/n87a4.pdf

Cormier, V.F. (2011). Seismic viscoelastic attenuation. In *Encyclopedia of Solid Earth Geophysics* (Vol. 53, pp. 1689–1699). Retrieved from: http://www.phys.uconn.edu/~cormier/encyclo_geophys_vfc.pdf

Cortés-Niño, A. & Sánchez-Tizapa, S. (2017). Elaboración de un mapa de isoperiodos para el Valle de Chilpancingo basándose en el análisis de microtremores. *Congreso Nacional de Ingeniería Sísmica*, 1, 1–16. Guadalajara, Jalisco, México.: Sociedad Mexicana de Ingeniería Sísmica.

Ehlen, J. (2002). Some effects of weathering on joints in granitic rocks. *Catena*, *49*(1–2), 91–109. https://doi.org/10.1016/S0341-8162(02)00019-X

García-Soto, A.D., Pozos-Estrada, A., Hong, H. & Gómez-Martínez, R. (2012). Estimacion del peligro sismico debido a sismos interplacae inslaby sus implicaciones en el diseño sismico. *Revista de Ingeniería Sísmica*, *54*(86), 27–54. Retrieved from: http://www.scielo.org.mx/pdf/ris/n86/n86a2.pdf

Johnston, D.H., Toksöz, M.N. & Timur, A. (1979). Attenuation of seismic waves in dry and saturated rocks: II. Mechanisms. *Geophysics*, *44*(4), 691–711. https://doi.org/10.1190/1.1440970

Ma'hood, M., Hamzehloo, H., & Doloei, G. J. (2009). Attenuation of high frequency P and S waves in the crust of the East-Central Iran. *Geophysical Journal International*, *179*(3), 1669–1678. https://doi.org/10.1111/j.1365-246X.2009.04363.x

Mártir-Mendoza, J.A. (2014). El gas de esquisto en la escena energética de México. *Juyyaania*, *2*(1), 141–159.

Morales-Corona, N. & Ramírez-Herrera, M.T. (2012). Técnicas histórico-etnográficas en la reconstrucción y caracterización de tsunamis: El ejemplo del gran tsunami del 22 de junio de 1932, en las costas del pacífico Mexicano. *Revista de Geografia Norte Grande*, 53, 107–122. Retrieved from: https://dialnet.unirioja.es/descarga/articulo/4778227.pdf

Núñez-Cornú, F.J., Ortiz, M. & Sánchez, J.J. (2008). The great 1787 Mexican tsunami. *Natural Hazards*, *47*(3), 569–576. https://doi.org/10.1007/s11069-008-9239-1

Okal, E.A. & Borrero, J.C. (2011). The "tsunami earthquake" of 1932 June 22 in Manzanillo, Mexico: Seismological study and tsunami simulations. *Geophysical Journal International*, *187*(3), 1443–1459. https://doi.org/10.1111/j.1365-246X.2011.05199.x

Perez-Gutierrez, R., Solari, L. a, Gomez-Tuena, A. & Martens, U. (2009). Mesozoic geologic evolution of the Xolapa migmatitic complex north of Acapulco, southern Mexico: implications for paleogeographic reconstructions. *Revista Mexicana De Ciencias Geológicas*, *26*(1), 201–221. Retrieved from: https://dialnet.unirioja.es/descarga/articulo/2936714.pdf

Quaas, R., Medina, S., Alcantara, L., Mena, E., Espinosa, J. M., Otero, J. A., … Munguía, L. (1996). Mexican Strong Motion Database. An integrated system to compile accelerograph data from the past 35 years. In Elsevier Science (Ed.), *Eleven World Conference on Earthquake Engineering* (pp. 1–8). Acapulco, México.

Raji, W. (2013). The use of seismic attenuation to indicate saturation in hydrocarbon reservoirs: Theoretical study and modelling approach. *Advances in Applied Science Research*, *4*(2), 45–53. Retrieved from: http://www.imedpub.com/articles/the-use-of-seismic-attenuation-to-indicate-saturation-in-hydrocarbonreservoirs-theoretical-study-and-modelling-approach.pdf

Sandoval, G.H., Alcántara, N.L., Arroyo, E.D., Delgado, D.M.R., Ordaz, S.M., Pérez, Y.C., … Ruiz, G. A.L. (2012). *Generación de mapas de intensidades sísmicas en tiempo real para el territorio nacional*, 1–7. Retrieved from: http://www.iingen.unam.mx/es-mx/BancoDeInformacion/BancodeImagenes/Documents/mapasdeintensidad.pdf

Singh, S.K., Mena, E., Castro, R. & Carmona, C. (1987). Empirical prediction of ground motion in Mexico City from coastal earthquakes. *Bulletin of the Seismological Society of America*, *77*(5), 1862–1867.

SSNMEX. (2018). Sismo del día 16 de febrero de 2018, Costa de Oaxaca (M 7.2). *UNAM*, pp. 1–14. UNAM.

Syed Mohsin, S.M., Ramli, N.I., Gul, Y., Al-Tawil, Y.M.Y. & Jokhio, G.A. (2018). Compressive and Flexural Tests on Adobe Samples Reinforced with Wire Mesh. *IOP Conf. Series: Materials Science and Engineering*, *318*, 012030. https://doi.org/10.1088/1757-899x/318/1/012030

Torres-Álvarez C.R. (2017). Efectos de Sitio en la Cd . de México durante el Sismo del 19 de septiembre de 2017. *Geotecnia*, *18*(246), 18–22. Retrieved from: https://issuu.com/smigorg/docs/revista-geotecnia-smig-numero-246

Tsige, M. & García Flórez, I. (2006). Propuesta de clasificación geotécnica del Efecto Sitio (Amplificación Sísmica) de las formaciones geológicas de la Región de Murcia. *Geogaceta*, (40), 39–42. Retrieved from: http://webs.ucm.es/info/tectact/DOCS/Articulos/Tsige_Geogaceta_2006.pdf

UIS-UNAM, CIS-IIGEN, & FCT-UALN. (2018). *Sismo de la Costa de Oaxaca (Mw7.2) 16 de febrero de 2018** (pp. 1–10). Instituto de Ingeniería, UNAM.

Völgyesi, L. (1982). The Inner Structure of the Earth. *Periodica Polytechnica Chem. Eng.*, *26*(3–4), 155–204. Retrieved from: https://pp.bme.hu/ch/article/view/2955/2060

Yamamoto, J., González-Moran, T., Quintanar, L., Zavaleta, A.B., Zamora, A. & Espindola, V. H. (2013). Seismic patterns of the Guerrero-Oaxaca, Mexico region, and its relationship to the continental margin structure. *Geophysical Journal International*, *192*(1), 375–389. https://doi.org/10.1093/gji/ggs025

GIS application software references

Blue Marble Geographics. (2015). Global Mapper v17.0.2. Hallowell, Maine 04347 U.S.A.

Environmental Systems Research Institute (ESRI). (2012). ArcGIS Release 10.1. Redlands, CA.